BRAGG REFLECTION OF COSMIC NEUTRINOS

By P. F. Smith and J. D. Lewin

Rutherford Appleton Laboratory, Chilton, Didcot, Oxon OX11 OQX, England

(Received June 19, 1984)

We discuss the possible applications of Bragg reflection in future detection schemes for low energy (and non-zero mass) cosmic neutrinos based on their coherent interaction with bulk matter. The reflection coefficient for laminated targets is shown to consist of two dominant parts arising from the mean and oscillating components of the target density, and the dependence of each of these terms on both the neutrino and target properties is discussed in detail. The Bragg reflection term provides an enhanced reflectivity for a selected band of neutrino wavelengths, which could be used to increase the detection sensitivity for cosmic neutrinos accelerated into the galaxy by its gravitational potential. For clustered neutrinos, we show that Bragg reflection would not increase the integrated coherent force, but could have experimental advantages in modulating and identifying the neutrino signal.

PACS numbers: 14.60.Gh, 95.85.Sz

1. Introduction

This paper relates to the coherent interaction of very low energy (cosmic or galactically-clustered) neutrinos with bulk matter, and to the possibility of future detection schemes based on this interaction.

In a previous paper [1] we discussed the reflection of low energy neutrinos by a finite-thickness plane slab of constant density, arriving at (second order) recoil forces of order 10^{-23} dyn/g for a typical estimated galactic flux of finite rest mass neutrinos ($m \simeq 20$ eV). In the present paper we discuss the possible experimental advantages of reflection from a target with spatially varying density, in particular an array of regularly spaced plates forming a 'Bragg mirror' for the incoming fermion waves. Such a target would have an enhanced reflection coefficient for a restricted band of neutrino wavelengths, and could have applications either as a 'tuned' detector or as a neutrino mirror capable of modulating or deflecting a significant fraction of the incident flux.

In Section 2 we examine the form of the backward scattering amplitude and reflection coefficient for a laminated target, and show that the reflected intensity contains two dominant terms corresponding to the mean and oscillating components of the target density. In Section 3 we discuss the properties of the mean density term, including the effect of the

characteristic 'penetration depth' and its dependence on neutrino rest mass. In Section 4, the properties of the oscillating density term are discussed, in particular the Bragg enhancement of the reflected wave for wavelengths corresponding to twice those of the Fourier components of the target density.

Possible practical applications of this selective reflection are discussed in Section 5, for both detection and modulation of the neutrino flux. In the case of extra-galactic neutrinos, accelerated by the galactic gravitational potential to give a low-momentum-spread flux through the solar system, large gains may be possible by the use of a tuned detector. For clustered galactic neutrinos we show that, for the expected broad band momentum distribution, Bragg reflection would not increase the total force per unit mass; it could, nevertheless provide an important degree of design flexibility, both in respect of identifying the signal and in determining the neutrino momentum and mass.

2. *Reflection from a target of varying density*

Finite mass neutrinos may of course be relativistic or non-relativistic. There is a significant difference in the form of the reflection amplitude for the two cases, which is discussed in detail in a separate paper [2]. We consider here the most experimentally interesting case of non-relativistic neutrinos, which includes both galactically-clustered neutrinos with

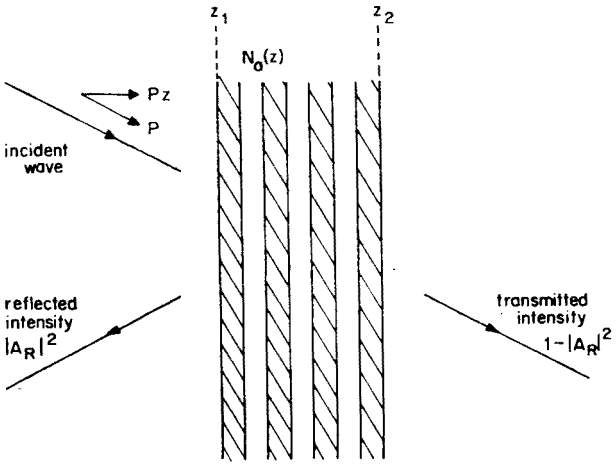

Fig. 1. Coherent scattering of neutrino wave from plane slab with z-dependent atomic density

$p \simeq 2\times10^{-2}$ eV, $m_\nu > 10^{-1}$ eV, and non-clustered cosmic background neutrinos with $p \simeq 5\times10^{-4}$ eV, $m_\nu > 10^{-3}$ eV.

Referring to Fig. 1, the first order (single scattering) reflected amplitude for a neutrino wave incident on a plane block of z-dependent density $\varrho_m(z)$ and/or atomic number $A(z)$ can be obtained by summation of spherical scattered wavelets for each elementary slab dz, giving the result [2]

$$A_R = [2\pi f(\pi)/k_z] \int_{z_1}^{z_2} N_a(z) e^{2ik_z z} dz, \tag{1}$$

where

$$N_a(z) = 6\times 10^{23}\varrho_m(z)/A(z) \quad \text{(atoms/cm}^3\text{)},$$

$$k_z = p_z/\hbar = 2\pi/\lambda_z \text{ (cm}^{-1}\text{)},$$

$$f(\pi) = f(0) = (4\sqrt{2}\,\pi)Gm_vN_2 \text{ (cm)},$$

$$\left.\begin{array}{rll} N_2 = Z-A & \text{for} & \nu_\mu, \nu_\tau, \ldots \\ \text{or } N_2 = 3Z-A & \text{for} & \nu_e \end{array}\right\} \text{ and opposite sign for } \bar{\nu}$$

and from (1) we can obtain the reflection coefficient

$$C = |A_R|^2. \tag{2}$$

Eq. (1) shows that the reflected amplitude depends on the Fourier coefficients of the atomic density fluctuation, giving a strong enhancement for incident momenta satisfying the usual Bragg condition $\lambda_z = \lambda_m/2$, where λ_m is the wavelength of the density fluctuations in the target. For a simple periodic system, such as a set of equally spaced plates, there are two dominant terms in (1) and (2), arising from the mean density (dc term) and the principal (usually the first) harmonic of the fluctuating density.

We illustrate this with a specific example. Consider a slab, infinite in x and y directions, with a sinusoidal atomic density variation, wavelength $\lambda_m = 2\pi/k_m$, in the z-direction:

$$N_a = N_{a0}[1+\sin k_m(z-z_0)] \tag{3}$$

extending from $z = z_0 - N\pi/k_m = z_0 - a/2$ to $z = z_0 + N\pi/k_m = z_0 + a/2$, where N is the number of complete periods and a is the total target thickness.

From (1) and (2) the reflection coefficient is

$$C = \frac{a^4}{4a_c^4}\,\frac{1}{k_z^2a^2}\left[\left(\frac{\sin k_za}{k_za}\right)^2 + \left(\frac{\sin k_sa}{2k_sa} - \frac{\sin k_da}{2k_da}\right)^2\right], \tag{4}$$

where

$$k_s = k_z + k_m/2, \quad k_d = k_z - k_m/2 \quad \text{and} \quad a_c^2 = \hbar^2/2m_vU \equiv [4\pi N_{a0}f(0)]^{-1}, \tag{5}$$

where U is the interaction potential [1] corresponding to the mean density. Eq. (4) divides naturally into two components: a "dc" term,

$$C_{dc} = \frac{a^4}{4a_c^4}\,\frac{1}{k_z^2a^2}\left(\frac{\sin k_za}{k_za}\right)^2, \tag{6}$$

which is the reflection coefficient we would obtain from (1) and (2) with constant atomic density $N_a = N_{a0}$; and an "ac" term,

$$C_{ac} = \frac{a^4}{4a_c^4}\,\frac{1}{k_z^2a^2}\left(\frac{\sin k_sa}{k_sa} - \frac{\sin k_da}{k_da}\right)^2, \tag{7}$$

which would result from an alternating atomic density $N_a = N_{a0}\sin k_mz$.

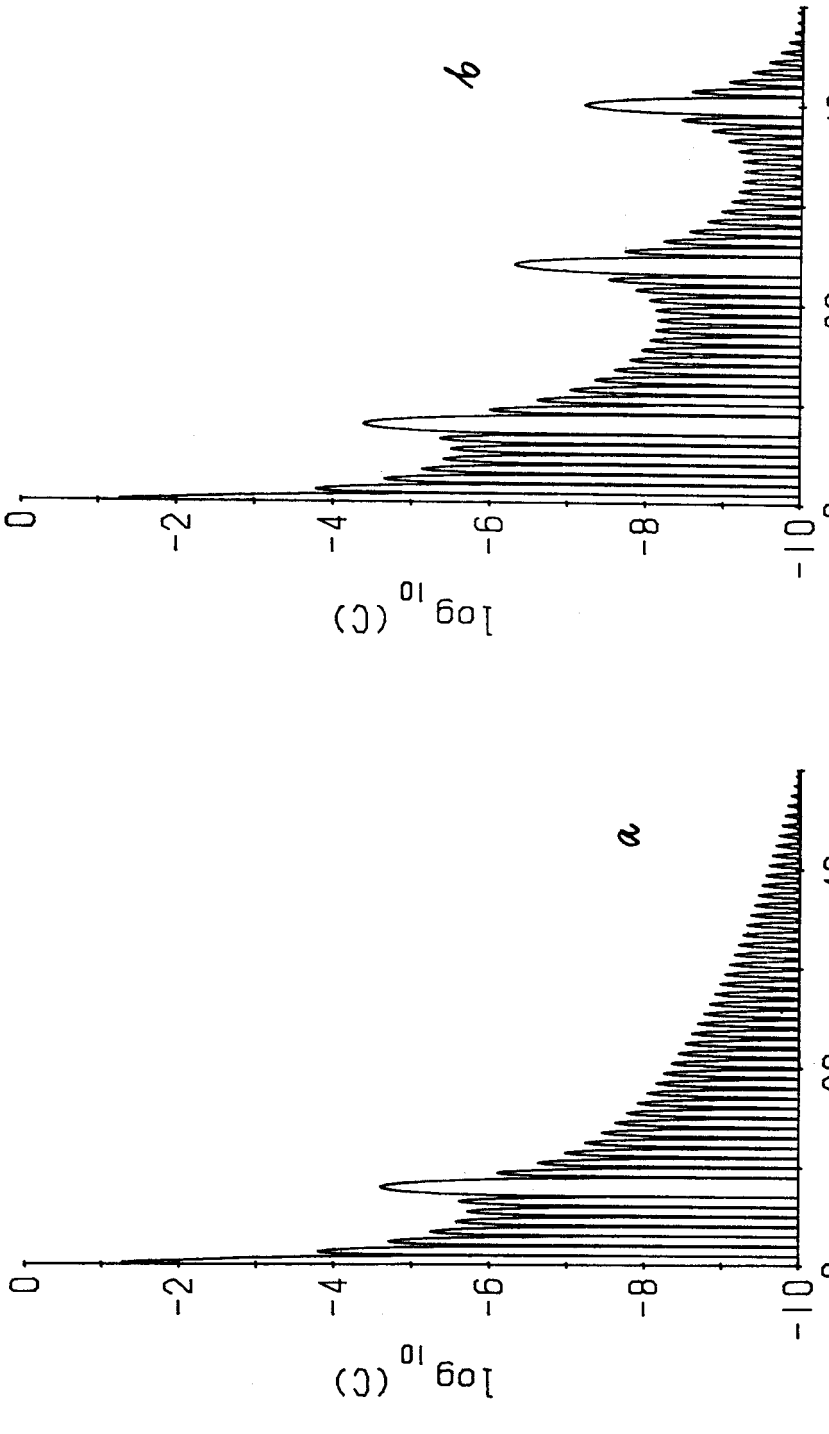

Fig. 2. Reflection coefficient versus $k_z a$ for periodic density variation with 8 complete periods: (a) Sinusoidal density variation; (b) Square wave density variation (equally spaced plates)

Fig. 2a illustrates the behaviour of (4) for $N = 8$. The peak at $k_z a \to 0$ arises from C_{dc}, and the 'Bragg' peak at $k_z a = 8\pi$ arises from the $(\sin k_d a)/k_d a$ term in C_{ac} (the term in k_s does not contribute significantly for k_z positive, but would give a similar peak at $k_z a = -8\pi$, corresponding to waves travelling in the negative z-direction). Fig. 2b shows a similar curve computed for the more realistic situation of a set of equally spaced plates. Here the square wave density variation gives rise to additional peaks corresponding to the odd harmonics in the Fourier expansion.

The relative importance of the two terms (6) and (7) depends on the incident neutrino momentum distribution and target geometry, and it is convenient first to consider the two contributions separately.

3. Reflection due to mean density term

For a block of constant density and thickness a (cm) the reflection coefficient is given exactly by [1]:

$$C_1 = \{1+[2n_z k_z^2 a_c^2/s(n_z k_z a)]^2\}^{-1}, \tag{8}$$

where

$$n_z^2 = |1-1/k_z^2 a_c^2|,$$

$$s(y) \equiv \sin(y) \quad \text{for} \quad 1/k_z^2 a_c^2 < 1 \text{ (i.e. } k_z^2 a_c^2 > 1 \text{ or } < 0),$$

$$s(y) \equiv \sinh(y) \quad \text{for} \quad 1/k_z^2 a_c^2 > 1$$

and, for $k_z a_c \gg 1$ (giving $C \ll 1$), (8) reduces to

$$C_2 \simeq [1/4k_z^4 a_c^4] \sin^2(k_z a) \tag{9}$$

which is, as expected, identical to C_{dc} (Eq. (6)).

Fig. 3 compares (8) and (9), showing C as a function of incident wavelength for various values of the target thickness. In general, the single scattering approximation is valid for $C \ll 1$, but is also still adequate up to $C \sim 0.3$ or higher, particularly if improved by the obvious substitution

$$C_2 \to (1+C_2^{-1})^{-1} \tag{10}$$

to prevent C exceeding unity. This comparison is of interest principally in providing an indication of the general accuracy of quantities derived with the single scattering approximation (1), such as C_{ac} (Eq.(7)), for which more exact expressions are not available.

The condition for (9) to be valid ($|k_z a_c| \gg 1$) is precisely the condition for n_z^2 - and hence C, to be insensitive to the sign of a_c^2 (and hence U and $f(0)$ – see Eq. (5)): physically, the reflection coefficient is the same for neutrinos and antineutrinos.

More specifically, if $|k_z a_c| > 1$, then $s(y) \equiv \sin(y)$ in (8), and C_1 has maxima

$$\hat{C}_1 = [1+(2n_z k_z^2 a_c^2)]^{-1} = (1-2k_z^2 a_c^2)^{-2}, \tag{11}$$

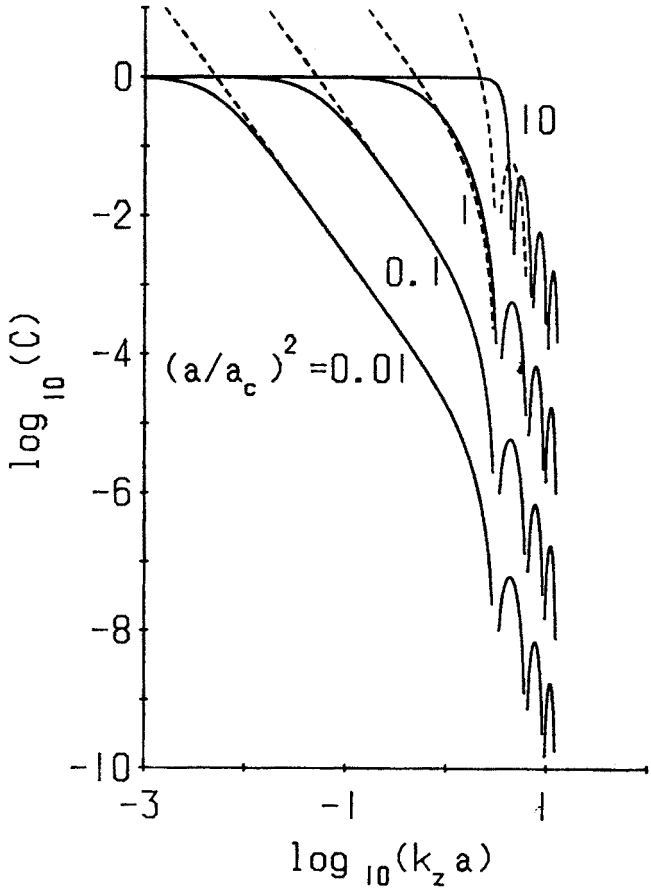

Fig. 3. Reflection coefficient versus k_z for block of constant density, and various constant values of thickness a. Full lines: exact formula (8); Dotted lines: single scattering approximation (9)

whenever $\sin(n_z k_z a) = 1$. Hence the peak reflection coefficients for positive and negative a_c^2 are in the ratio

$$\frac{\hat{C}_1(a_c^2 < 0)}{\hat{C}_1(a_c^2 > 0)} = \left(\frac{1-2|k_z^2 a_c^2|}{1+2|k_z^2 a_c^2|}\right)^2, \tag{12}$$

which lies between 0.8 and 1 for $|k_z^2 a_c^2| > 10$.

However, for $|k_z^2 a_c^2| < 3$, significant differences between neutrinos and antineutrinos appear. This is illustrated in Fig. 4, where (8) is plotted as a function of target thickness for fixed incident wavelength and both signs of a_c^2.

The region where particle and antiparticle coefficients are clearly distinguishable – i.e., very roughly, $C > 0.01$ – is also of interest in providing, in principle, an elegant method of estimating a_c^2 and hence the neutrino mass (or masses) through (5), by measuring the reflection force per unit volume as a function of target thickness. In practice, however,

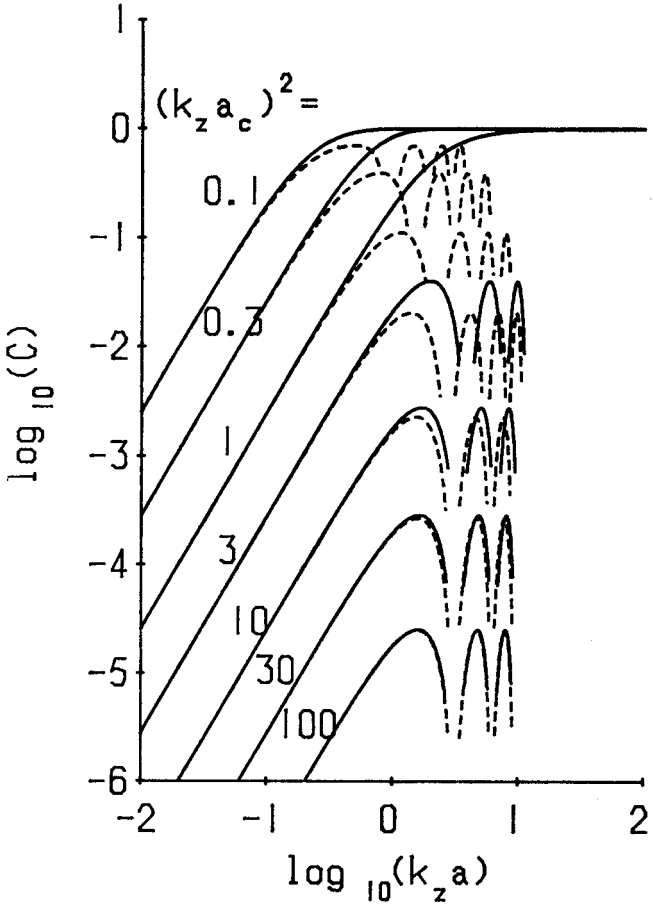

Fig. 4. Reflection coefficient versus target thickness for block of constant density and various constant values of incident wavelength. Full lines: positive $a_c^2(\nu_e, \bar{\nu}_\mu, \bar{\nu}_\tau \ldots)$. Dotted lines: negative $a_c^2(\bar{\nu}_e, \nu_\mu, \nu_\tau \ldots)$

both of these subtle effects, predicted on the basis of a transversely infinite target, are likely to be masked by the influence of finite target end effects at low incident momenta. These and other ways of estimating the cosmic neutrino masses will be considered in a separate paper.

Note that, in both Fig. 3 and Fig. 4, the oscillatory behaviour for $1/k_z^2 a_c^2 < 1$ depends on the coherence between front and back surfaces, and would be smoothed out if the surfaces were irregular or 'rough' on the scale of a wavelength (e.g. of order 60 microns for the expected mean momentum of galactically clustered neutrinos). In practice, also, C must be integrated over the momentum spectrum of the incident flux, which (unless itself selected by a 'Bragg mirror' as discussed below) would invariably have sufficient bandwidth to render the oscillatory behaviour unobservable.

4. Reflection due to harmonic term

We now consider the "ac" contribution to C, given by (7). Since

$$k_s a = k_z a + N\pi$$

and

$$k_d a = k_z a - N\pi,$$

only the term in $k_d a$ is important if $N > 1$. (If $k_z a \ll N\pi$, so that the two terms are comparable, $C_{ac} \ll C_{dc}$.) We write this term:

$$C(k_z) = C_k \frac{\sin^2 k_d a}{k_d^2 a^2}, \tag{13}$$

where

$$C_k = \frac{a^4}{16 a_c^4} \frac{1}{k_z^2 a^2} = \left(\frac{a}{4 k_z a_c^2}\right)^2. \tag{14}$$

The peak value of (13), C_0, occurs when $k_d = 0$, i.e. when k_z has the Bragg value

$$k_b = N\pi/a \quad (= k_m/2), \tag{15}$$

and is given by

$$C_0 = C_k(k_z = k_b) = \left(\frac{N\pi}{4 k_b^2 a_c^2}\right)^2 = \left(\frac{a^2}{4 N\pi a_c^2}\right)^2, \tag{16}$$

where we have chosen to show explicitly the N dependence of C_0 according to whether one fixes wavelength (i.e. k_b) or target thickness.

For $N \gg 1$ it is convenient to define a width Δk for the reflection peak by:

$$\Delta k = \frac{1}{C_0} \int_{k_b - q\pi/a}^{k_b + q\pi/a} C(k_z) dk_z, \tag{17}$$

where $1 \ll q \ll N$ (so that the integration takes in the peak at k_b) giving

$$\Delta k \simeq \pi/a = k_b/N \tag{18}$$

(since $C_k \simeq$ constant $\simeq C_0$ for $\Delta k \ll N\pi/a$, i.e. for $N \gg 1$).

For practical purposes we are interested in the force on the slab, given by the product of momentum transfer (i.e. the momentum reversal), incident flux, and reflection coefficient:

$$F/A \,(\mathrm{dyn/cm^2}) = \int_0^\infty 2\hbar k_z \phi_z(k_z) C(k_z) dk_z, \tag{19}$$

where $\phi_z(k_z)$ is the spectrum of incident flux perpendicular to the slab.

For an incident flux of low momentum spread, (19) will be maximized by choosing a and N to match $C(k_z)$ to the incident momentum and bandwidth. A possible example of this will be discussed in Section 5. For a broad band flux, such as that due to motion through a clustered galactic distribution, the behaviour of (19) requires more detailed examination.

For a hypothetical distribution of galactic neutrinos with number density:

$$d\varrho_\nu(k) = \varrho_\nu \pi^{-3/2} k_0^{-3} \exp(-k^2/k_0^2) d^3k \tag{20}$$

the total perpendicular flux (from one hemisphere) is given by

$$\phi_z(k_z)dk_z = (\hbar k_z/m_\nu)(\varrho_\nu \pi^{-1/2}/k_0) \exp[-(k_{sz}-k_z)^2/k_0^2]dk_z, \tag{21}$$

where $k_s = m_\nu v_s$, v_s = galactic orbital velocity, and k_{sz} is the component of k_s perpendicular to the surface.

For $k_z < k_0$ and $k_s \simeq k_0$, the exponential factor lies between 1 and e^{-1} and for simplicity can be ignored in illustrative calculations. Integrating (19) with (13) and (20) then gives, denoting the neutrino Compton wavelength $\hbar/m_\nu c$ by l_ν:

$$F_1/A\ (\mathrm{dyn/cm^2}) = (\pi^{1/2}\varrho_\nu/8k_0a_c)(l_\nu/a_c)^3 (m_\nu c^2/l_\nu)a \tag{22a}$$

and hence

$$F_1/V\ (\mathrm{dyn/cm^3}) = (\pi^{1/2}\varrho_\nu/8k_0a_c)(l_\nu/a_c)^3 (m_\nu c^2/l_\nu) \tag{22b}$$

from which it is seen that the force per unit volume is constant, i.e. dependent on the target material and incident particle properties (via m_ν, a_c, and k_0) but independent of the choice of N and a. From (16), (18) and (22b), we see that increasing N (at fixed λ_m) makes the reflection peak stronger and narrower, the resulting value of F/V remaining constant. Similarly C_0 may be increased by decreasing k_b, but the compensating reductions in momentum transfer and flux (via the reduced velocity) result in a constant value for (22b). Note that, for galactic neutrinos with $m_\nu = 20$ eV, typical values for the quantities in (22) would be $l_\nu \simeq 10^{-6}$ cm, $a_c \simeq 6$ cm, $1/k_0 \simeq 10^{-3}$ cm, $\varrho_\nu \sim 2 \cdot 10^7\ \mathrm{cm^{-3}}$.

The preceding discussion for the sinusoidal atomic density variation (3) can be generalized to more realistic practical configurations by writing the target density as a Fourier series:

$$N_a = N_{a0}[1 + \sum_n b_n \cos nk_m z] \tag{23}$$

for which (13) is replaced by

$$C(k_z) = C_k \sum_n \left(\frac{b_n^2 \sin^2 k_{dn}a}{4k_{dn}^2 a^2}\right) \tag{24}$$

(where $k_{dn} = k_z - nk_b$) and the total force arising from all of the harmonic terms is, in place of (22), given by

$$F_H = F_1 \sum_n b_n^2. \tag{25}$$

For the example of a set of solid plates, with separation equal to thickness, the harmonic coefficients of the square wave give simply

$$F_H = 2F_1. \tag{26}$$

The overall force on the target is (25) plus the force F_0 arising from the mean density term. This is obtained by evaluating (19) with $C(k_z) = C_2$ from (9), giving the result:

$$F_0 = 2F_1 \tag{27}$$

and the total force per unit volume:

$$F_T/V = (F_0+F_H)/V = 4F_1/V. \tag{28}$$

This is a particular case of the more general possibility of an array of equally spaced plates occupying a fraction f of the target volume, i.e. with a thickness/separation ratio $f/(1-f)$. This is represented by the Fourier series:

$$N_a = N_{a0}\left[1+\sum_n \frac{2\sin fn\pi}{fn\pi}\cos nk_m z\right] \tag{29}$$

with

$$N_{a0} = fN_a\,(\text{peak}), \tag{30}$$

Defining a quantity D, involving the incident flux parameters, by

$$D = \pi^{1/2}\varrho_v\hbar^2/4m_v k_0 \tag{31}$$

we see from (22) and (25) that the total force is given by

$$F_T/V = (D/a_c^4)\,(1+\tfrac{1}{2}\textstyle\sum b_n^2) \tag{32}$$

which, with (29), becomes

$$F_T/V = (D/a_c^4)\left(1+\frac{1-f}{f}\right) \tag{33}$$

$$= D/fa_c^4 \tag{34}$$

which increases with decreasing f. However, the mechanical response of the target is governed by the force per unit mass:

$$F/M = F/V \times 1/\varrho_{m0} = D(fa_c^4\varrho_{m0})^{-1} \tag{35}$$

(where ϱ_{m0} is the mean value of the material density ϱ_m) and since, from (5), $a_c^2 \propto U_m^{-1}$ $\propto (U_1\varrho_{m0})^{-1}$, where U is the potential for unit density, it can be seen that the value of (35) is in fact independent of f and proportional simply to the peak density of the structure ϱ_{m0}/f.

5. *Applications*

As an illustration of the use of the preceding theory, we consider two possible applications to coherent neutrino detectors, one relating to a narrow band flux and the other to a broad band flux. It might at first appear that there would be no examples of a narrow band cosmic neutrino flux, since whether the relic neutrino background is (a) uniformly distributed, or (b) clustered in the galaxy, one expects an approximately uniform population in momentum space up to some characteristic value p_0 (of order 5×10^{-4} eV for (a) and 2×10^{-2} eV for (b)). However, for neutrinos of finite mass, the galaxy represents a gravitational potential well, and, as the galaxy moves through the type (a) background, the neutrinos are accelerated into and through the galaxy by the potential, producing a flux of higher average momentum but with its original momentum spread essentially unchanged.

The potential V_s at the position of the solar system is approximately[1]:

$$-V_s(\text{eV}) = 2.4 \times 10^{-6} m_\nu(\text{eV}) \tag{36}$$

We consider a neutrino of initial momentum $\boldsymbol{p}$ relative to the cosmic microwave background, and thus with a momentum $\boldsymbol{p}_r$ relative to the galaxy given by

$$\boldsymbol{p}_r = \boldsymbol{p} + m_\nu \boldsymbol{v}_g, \tag{37}$$

where $\boldsymbol{v}_g$ is the velocity of the galaxy relative to the microwave background, $\simeq 1.7 \times 10^{-3}\, c$. The increased momentum p_s at the solar system is given by

$$p_s^2 = [(p_r^2 + m_\nu^2)^{1/2} + V_s]^2 - m_\nu^2. \tag{38}$$

The initial momentum p is expected to have a red-shifted Fermi distribution of average momentum $p_0 \simeq 5 \times 10^{-4}$ eV, and the above equations then show that for $m_\nu < 0.1$ eV (i.e. $p > m_\nu v_g$ in (37)), $p_s \simeq p_r \simeq p$ and the galactic potential has little effect on the momentum distribution, but for $m_\nu > 0.3$ eV (i.e. $m_\nu v_g > p$ in (37)) the momentum is increased by the gravitational potential to $p_s \simeq 3 \times 10^{-3}\, m_\nu\,(\text{eV})$ while the momentum spread remains approximately independent of m_ν at $\Delta p_s \simeq 0.6\, \Delta p_r \simeq 1.2 p_0 \simeq 6 \cdot 10^{-4}$ eV.

Thus, for the non-clustered cosmic neutrino flux passing through the solar system, we have the following estimates for the fractional momentum spread:

$$f_i = \left(\frac{\Delta k}{k}\right)_g = \left(\frac{\Delta p}{p}\right)_g \sim 1 \quad (m_\nu < 0.1 \text{ eV}) \tag{39}$$

or

$$\sim \frac{0.2}{m} \quad (m_\nu > 0.3 \text{ eV}) \tag{40}$$

---

[1] Estimated from the three-component model of Caldwell and Ostriker [3], which gives approximate contributions 0.6×10^{-6} m_ν from the visible matter ('disc' + 'spheroid') and 1.8×10^{-6} m_ν from the dark matter ('halo'). The total corresponds to a galactic escape velocity of about $6 \cdot 10^7$ cm s^{-1}.

TABLE I

Illustrative figures for a detector of thickness $a = 30$ cm (bandwitdh in eV $= 2 \cdot 10^{-5}\,\pi/a$), tuned to various 'slices' of the incident momentum distribution by varying the lamination wavelength λ_m. The incident flux figures correspond to typical 'clustered galactic' values [1] with $m_\nu = 20$ eV, $p < 2 \cdot 10^{-2}$ eV, ϕ calculated for a dark matter density $\sim 10^{-24}$ g cm^{-3} (number density $\varrho_\nu \sim 2 \cdot 10^7$ cm^{-3}). The reflection coefficient C is that for the 1st harmonic periodic density term only

Incident neutrino flux					Detector, $a = 30$ cm			
p_z	k_z	λ_z	v/c	$d\phi_z/dp_z$	λ_m	N	dp_d	C
eV	cm^{-1}	cm		cm^{-2} eV^{-1}	cm		eV	
$2 \cdot 10^{-2}$	10^3	$6 \cdot 10^{-3}$	10^{-3}	10^{16}	$3 \cdot 10^{-3}$	10^4	$2 \cdot 10^{-6}$	$4 \cdot 10^{-8}$
$2 \cdot 10^{-3}$	10^2	$6 \cdot 10^{-2}$	10^{-4}	10^{15}	$3 \cdot 10^{-2}$	10^3	$2 \cdot 10^{-6}$	$4 \cdot 10^{-6}$
$2 \cdot 10^{-4}$	10	0.6	10^{-5}	10^{14}	0.3	10^2	$2 \cdot 10^{-6}$	$4 \cdot 10^{-4}$
$2 \cdot 10^{-5}$	1	6	10^{-6}	10^{13}	3	10	$2 \cdot 10^{-6}$	.04
$1 \cdot 10^{-5}$	0.5	12	$5 \cdot 10^{-7}$	$5 \cdot 10^{12}$	6	5	$2 \cdot 10^{-6}$	.16
$4 \cdot 10^{-6}$	0.2	30	$2 \cdot 10^{-7}$	$2 \cdot 10^{12}$	15	2	$2 \cdot 10^{-6}$	~ 1

From (15), a periodic detector has $f_d = (\Delta k/k)_d \simeq 1/N$ and, provided that $N \geqslant f_i^{-1}$, the force per unit area resulting from Bragg reflection is proportional to a/f_i. We conclude that, in principle, the force per unit volume can be increased by the use of a 'tuned' target by a factor f_i^{-1}, which, from (40), may be one or two orders of magnitude if $2 < m_\nu < 20$ eV.

A further gain in sensitivity may be possible as a result of the fact that this gravitationally-accelerated flux would be peaked in the direction of the galactic centre, and a non-isotropic flux of this type could in principle be partially focused or concentrated by, for example tuned cylindrical 'neutrino guides' (somewhat analogous to those used in neutron optics [4]). High density material lenses, with or without Bragg wavelength selection, are a further possibility, remembering that the length of optical systems scales as $(n-1)^{-1} \sim 10^4$ for 10^{-2} eV neutrinos, and the construction of kilometer length focusing systems should be perfectly feasible.

For the broad band case $\Delta p/p \sim 1$, as is expected for the clustered galactic flux, we have seen that a laminated target gives, for fixed k_b, a reflection coefficient proportional to N^2 for $1/N$ of the incident flux and N times the target volume. Thus the force per unit volume is independent of N and no gain in sensitivity results. This constancy of F/V also results at fixed target thickness, and we illustrate this by means of the typical values in Table I, which shows the effect of varying N in a stack of detector plates of total thickness 30 cm, to produce Bragg reflection for various values of incident momentum. It is seen that C varies as $1/p_z^2$ while the product $C(d\phi/dp)pdp$, which is proportional to F/V, remains constant.

The figures in Table I suggest that, although there is no absolute gain in sensitivity, the use of Bragg reflection could provide an important degree of freedom in the design of the detector. In particular one might tune the detector to a low value of the incident momentum in order to obtain a higher value for the reflection coefficient, allowing the experimental option of screening the apparatus with a system of similarly tuned Bragg reflectors,

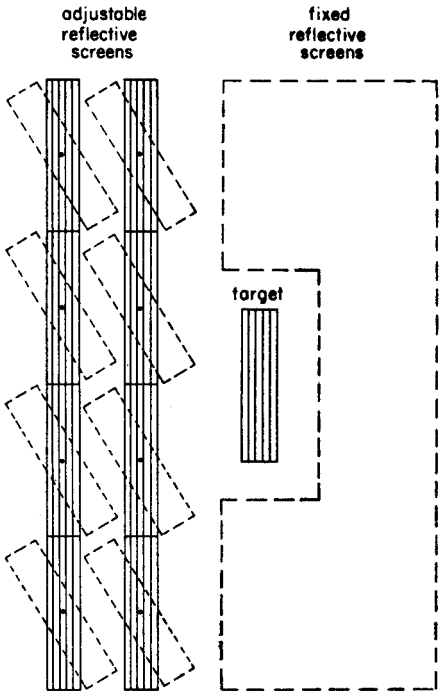

Fig. 5. Schematic illustration of possible scheme using Bragg mirrors to modulate the flux of low energy neutrinos on a tuned target (note that diagram is not to scale — ratio of transverse to longitudinal dimensions may be several orders of magnitude)

some of which could be periodically opened or de-tuned (for example like a venetian blind) to produce a significant modulation of the neutrino flux (Fig. 5). This could be of crucial importance firstly in identifying the signal and secondly in converting the essentially dc force to the more measurable form of a periodic force of precisely known frequency. Note however, from (21), that the difference in flux (within a momentum range dk_z) incident from the left and right hand hemispheres is proportional to $\exp(2k_{sz}k_z/k_0) - \exp(-2k_{sz}k_z/k_0)$, i.e. to $\sinh(2k_{sz}k_z/k_0)$, which shows that the flux of low-k_z neutrinos seen by the target becomes effectively isotropic, despite the asymmetry produced by the galactic velocity component k_{sz}/m_ν. In turn this means that a single reflecting screen will not produce any modulation, since in the closed position it will reflect an equivalent flux originating from the right hand hemisphere in Fig. 5. In this situation it would be necessary to devise a set of screens which will create an anisotropic flux at the target, for example by isolating the two hemispheres with high reflectivity barriers. In principle, reflection coefficients and modulation levels approaching 100% could be achieved with multiple screens. Unfortunately, a simple increase in thickness a_s (giving $C \propto a_s^2$) is not appropriate, since the screened bandwidth will decrease as $1/a_s$. Instead, a number n_s of screens of the desired bandwidth can be placed in series, with small separations (e.g. of order λ/n_s) chosen to destroy the phase coherence. This will achieve a constant bandwidth, but with C now increasing only linearly with n_s.

A similar principle applies to the design of concave Bragg mirrors, which might also be considered as possible concentration or modulation elements. A basic mirror thickness must first be chosen to give the required bandwidth, and the reflectivity then increased by combining additional elements incoherently.

The feasibility of ideas of this type clearly depends on the extent to which the one-dimensional approximation (effectively infinite width slabs) can be realized in practice, since the constancy of F/V with decreasing p_z, and the corresponding flux modulation ideas, depend on the utilization of flux incident at very small angles α to the plate surface ($\alpha \simeq p_z/p_0$), and this in turn would appear to require the use of detecting plates and/or modulating mirrors of correspondingly large width/thickness ratio (e.g. 10^3–10^4). It is also evident from this that the dependence of the coherent force on the acceptance angle of the system would provide, in principle, a method of measuring p_z/p_0, hence giving p_0 and, by inference, m_ν (since p_0/m_ν for clustered neutrinos must be of the same order as the velocity dispersion of the galaxy). Some computational studies of the properties of finite detector configurations with smaller aspect ratios (1–10^2) are in progress.

The problems associated with the measurement of the forces on the slab will be discussed separately; but in general terms it is envisaged that the tuned detector slab would be levitated in a low temperature, ultra-high vacuum enclosure, with the small displacements (relative to a neighbouring untuned target) measured by optical or electromagnetic techniques analogous to those under development for gravitational wave detection [5]. Many aspects of the system, including the very large transverse/longitudinal dimension ratio, would suggest that a zero-g (orbital) enviromnent may be the most appropriate for future experiments of this type.

REFERENCES

[1] P. F. Smith, J. D. Lewin, *Phys. Lett.* **127B**, 185 (1983).
[2] P. F. Smith, *Nuovo Cimento* A (to be published).
[3] J. A. R. Caldwell, J. P. Ostriker, *Astrophys. J.* **251**, 61 (1981).
[4] See, for example, A. G. Klein, S. A. Werner, *Rep. Prog. Phys.* **46**, 259 (1983); G. E. Bacon, *Neutron Physics*, Wykeham publications 1969, p. 123.
[5] See, for example, V. B. Braginsky, A. B. Manukin, *Measurement of weak forces in physics experiments*, University of Chicago Press, Chicago 1977; K. S. Thorne, *Rev. Mod. Phys.* **52**, 285 (1980); R. W. F. Drever, *Quart. J. R. Astron. Soc.* **18**, 9 (1977); R. Weiss, in *Sources of Gravitational Radiation*, Cambridge University Press, 1979, p. 7; E. Amaldi, in Proc. 2nd Marcel Grossman Meeting on General Relativity, Vol. 1, North Holland 1982, p. 21.